iScience

CellPress
OPEN ACCESS

Article

Transforming the CRISPR/dCas9-based gene regulation technique into a forward screening tool in *Plasmodium falciparum*

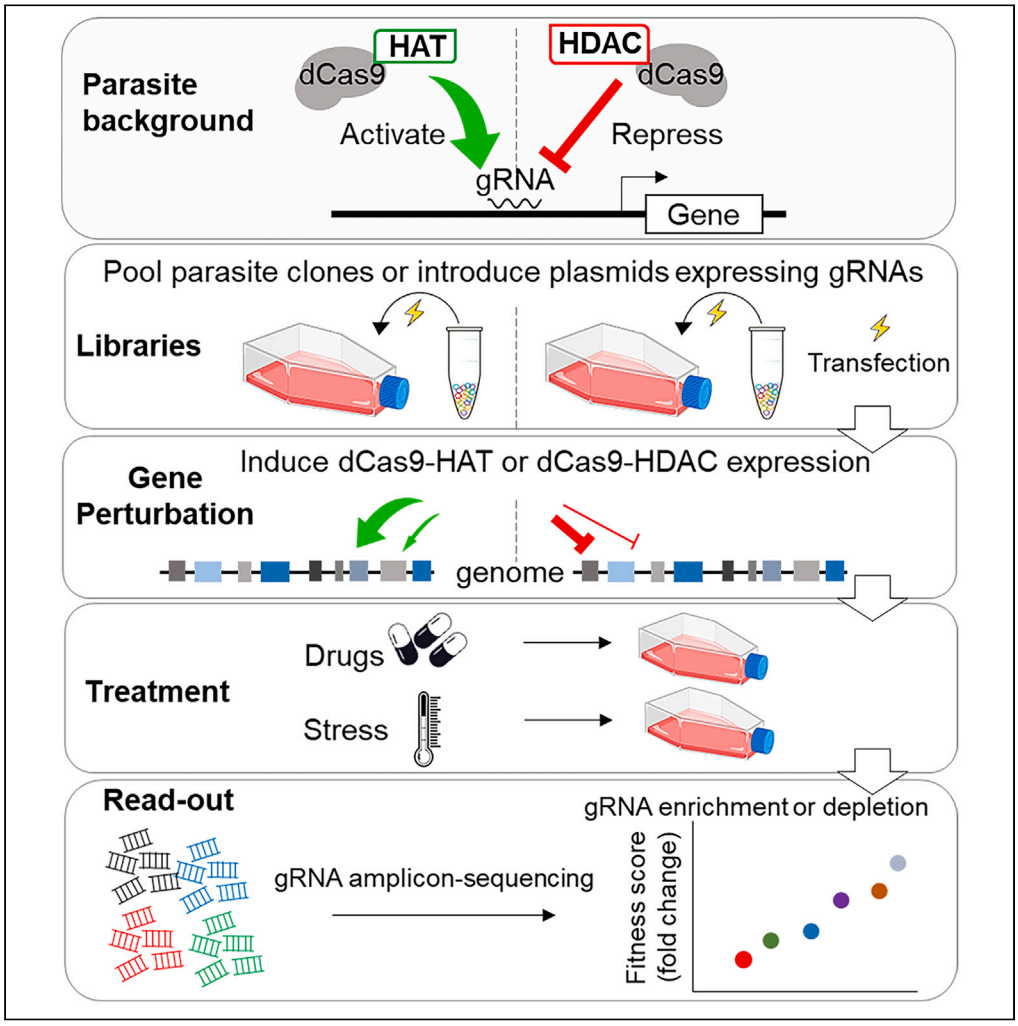

Amuza Byaruhanga Lucky, Chengqi Wang, Xiaolian Li, Xiaoying Liang, Azhar Muneer, Jun Miao

jmiao1@usf.edu

Highlights

CRISPR interference-/activation-based screening system was assessed in *P. falciparum*

The system was easily built by a single transfection for studying essential genes

This screening identified genes contributing to various drug and stress treatments

The system was reproducible, straightforward, and robust in *P. falciparum*

Lucky et al., iScience 27, 109602
April 19, 2024
https://doi.org/10.1016/j.isci.2024.109602

iScience

CellPress
OPEN ACCESS

Article

Transforming the CRISPR/dCas9-based gene regulation technique into a forward screening tool in *Plasmodium falciparum*

Amuza Byaruhanga Lucky,[1,4] Chengqi Wang,[2,4] Xiaolian Li,[1] Xiaoying Liang,[1,3] Azhar Muneer,[1] and Jun Miao[1,2,5,*]

SUMMARY

It is a significant challenge to assess the functions of many uncharacterized genes in human malaria parasites. Here, we present a genetic screening tool to assess the contribution of essential genes from *Plasmodium falciparum* by the conditional CRISPR-/deadCas9-based interference and activation (i/a) systems. We screened both CRISPRi and CRISPRa sets, consisting of nine parasite lines per set targeting nine genes via their respective gRNAs. By conducting amplicon sequencing of gRNA loci, we identified the contribution of each targeted gene to parasite fitness upon drug (artemisinin, chloroquine) and stress (starvation, heat shock) treatment. The screening was highly reproducible, and the screening libraries were easily generated by transfection of mixed plasmids expressing different gRNAs. We demonstrated that this screening is straightforward, robust, and can provide a fast and efficient tool to study essential genes that have long presented a bottleneck in assessing their functions using existing genetic tools.

INTRODUCTION

With ~249 million cases and 608,000 deaths in 2022,[1] malaria continues to pose a significant global health burden. With the currently available malaria vaccine's low efficacy[2] and the spread of artemisinin resistance,[3–6] the need for novel therapeutic innovations cannot be overemphasized. The rational design of effective vaccines, drugs, and diagnostic tools must be guided by clear insights into the precise functions of individual gene products. Efforts focused on understanding the functions of essential genes in *Plasmodium falciparum* can be aided by developing new molecular tools, given that the current tools, such as randomly mutating the genome by chemicals or transposition, are challenging as attaining saturation is laborious and essential genes cannot be directly mutated.[7,8]

In the past decade, the application of CRISPR-based genetic screens via genome-wide mutation, transcriptional interference or inactivation (CRISPRi), and activation (CRISPRa) have greatly transformed the way we understand cellular biology, gene essentiality, and drug resistance mechanisms in a variety of model organisms[9–15] and particularly in apicomplexan parasites.[16,17] To date, CRISPR genome-wide mutation screens have only been reported in *Toxoplasma*.[16] This is majorly attributed to the presence of the canonical non-homologous end-joining (c-NHEJ) pathway, which makes CRISPR more feasible in *T. gondii* than in *Plasmodium and Leishmania*.[18] Approximately 40% of *T. gondii* genes significantly contribute to parasite fitness (essential genes). Among these, ~200 protein-coding genes were functionally unknown and conserved in the apicomplexan parasites.[16] Targeted CRISPR screens have also been utilized to determine gene functions in *T. gondii*'s specific *in vivo* fitness.[17,19–22] Recently, more innovative CRISPR screens have been conducted in *T. gondii* to define the functional roles of genes involved in host egress and invasion,[23] as well as the kinome.[24] Even more recently, a CRISPR/Cas9 cytosine base editor (CBE) was successfully used in *Leishmania* to deplete genes by creating a stop codon, and for the first time, a small-scale screen was performed, demonstrating that this system is feasible for viability screening of essential genes.[25] A position-dependent reduction in gene expression was found when CRISPR interference (CRISPRi) was applied in *Plasmodium yoelii* by guiding the catalytically dead SpCas9 (dSpCas9) to the upstream of a target gene.[26] To date, ~50%–60% of *P. falciparum* protein-coding genes are essential to ensure successful parasitism,[8,27] yet only a handful of them have biological roles explicitly defined.[28,29] The current knowledge gap in *Plasmodium* gene function poses a significant challenge in the development of effective malaria vaccines and drugs. To address this gap, we aimed to expand the tool kit to aid in studying *Plasmodium* essential gene functions.

CRISPR-mutagenesis screens in *Plasmodium* are challenging due to the absence of c-NHEJ and the repetitive AT-rich genome.[18] Furthermore, a CRISPR study using microhomology-mediated end joining as an alternative pathway in *P. falciparum* revealed inherent challenges.[30] To address all these challenges, we successfully developed an inducible CRISPR/deadCas9 (dCas9) regulation system through the fusion of

[1]Department of Internal Medicine, Morsani College of Medicine, University of South Florida, 3720 Spectrum Boulevard, Tampa, FL 33612, USA
[2]Center for Global Health and Infectious Diseases Research, College of Public Health, University of South Florida, 3720 Spectrum Boulevard, Tampa, FL 33612, USA
[3]Present address: Department of Molecular Oncology, Moffitt Cancer Center, 12902 USF Magnolia Drive, Tampa, FL 33612, USA
[4]These authors contributed equally
[5]Lead contact
*Correspondence: jmiao1@usf.edu
https://doi.org/10.1016/j.isci.2024.109602

dCas9 with two epigenetic modifiers, namely, PfSir2a as a repressor (a histone deacetylase; HDAC) and PfGCN5 as an activator (a histone acetyltransferase; HAT).[31] In this study, we have utilized our inducible CRISPR-/dCas9-based CRISPRi/a system to perform a small-scale phenotypic screening of genes from mixed parasite pools. In contrast to individual gene screening, pooled screening enables the simultaneous comparison of all targeted genes, allowing for the detection of subtle defects that may only be apparent in competitive contexts and the identification of the genes involved in stress or drug responses. This study for the first time demonstrates that the CRISPRi/a pooled screening approach is a simple, robust, and resourceful tool for defining the functions of essential genes in *P. falciparum*.

RESULTS

The inducible CRISPRi/a screens genes that impact fitness in standard culture conditions

Given the incredible versatility and usefulness of CRISPRi/a in other organisms,[9–17] we wanted to evaluate the potential of the newly established inducible CRISPRi/a systems for forward screening purposes in *P. falciparum*.[31] We speculate that if manipulating the expression of individual genes in *P. falciparum* affects their functions, the effect would be reflected in the fitness of the parasites, which can be revealed in pooled growth competition analysis. To test this hypothesis, we pooled two sets of parasite lines that repress (CRISPRi or dCas9-HDAC) or activate (CRISPRa or dCas9-HAT) nine genes by their respective and unique gRNAs. Each set consisted of pooled parasites from the nine parasite lines generated in the initial conditional CRISPRi/a study targeting eight genes (*ATG18, AP2G, CHC, CRT, DNMT, GCN5, K13,* and *MYST*)[31] and the current study targeting *MDR1* by introducing a specific gRNA into dCas9-HDAC and dCas9-HAT parasite lines (Figure S1A, Table S1). We named each parasite line by the targeted gene name and its dCas9 background (HDAC or HAT), such as *ATG18*-HAT standing for a parasite line with a gRNA targeting *ATG18* in the inducible dCas9-HAT background. dCas9-HDAC or HAT pools were made by combining equal numbers of synchronized parasites. Expression of the dCas9-HDAC or dCas9-HAT was induced by adding rapamycin (+rap) to the pooled parasite culture overnight at the early ring stage (Figure 1A). Non-induced parasite cultures (−rap) were used as controls. The parasite populations were sampled at six time points over 11 days, with each sampling occurring every intraerythrocytic developmental cycle (IDC) which is ∼48 h. Genomic DNA was isolated from the samples, and PCR was performed to amplify the gRNA loci, which were then barcoded for amplicon deep sequencing within a single sequencing reaction (Figure 1B). The sequencing reads were mapped to known gRNA sequences. Similar to the CRISPR/Cas9 CBE screen,[25] the number of specific gRNA reads was used to calculate the relative abundance of the parasites carrying that gRNA in the pool. The abundance of each gRNA on a specific day was used to compare its abundance on day 0 (t_0) of induction (+rap) to quantify the variation of each parasite population during the culture process (Figure 1A, Table S2).

Our earlier study showed that individually repressing or activating the abovementioned eight target genes by specific gRNAs in dCas9-HDAC or -HAT background did not result in noticeable growth changes except that upregulation of *ATG18* and *AP2G* in *ATG18*-HAT and *AP2G*-HAT led to a growth defect and an increased commitment to gametocytogenesis, respectively.[31] We did not monitor the growth phenotype for *AP2G*-HDAC in our earlier study because *AP2G* was considered a silenced gene during IDC.[31] Up- or downregulation of *MDR1* in *MDR1*-HDAC or *MDR1*-HAT with gRNA 1 also did not result in noticeable growth defects (Figures S1B–S1D). We thus anticipated that there would be minimal changes in the relative abundance of each gRNA within each pooled set without rap induction (−rap), and the abundance of gRNAs in *ATG18*-HAT and *AP2G*-HAT would be reduced in the pooled set after induction (+rap). Indeed, without rap induction (−rap), the relative abundance of each gRNA in the pools remained relatively stable (<2-fold) for the first 2 IDCs; however, after the third IDC, the alterations gradually elevated at a relatively low level (Figures S2A and S2B). In contrast, upon induction (+rap), the alteration of the relative abundance of each gRNA was higher than the control (−rap), especially at late time points (Figures S2C and S2D). By directly comparing the abundance of each gRNA between the induced libraries (+rap) and their respective controls (−rap), we observed significant alterations after induction and these alterations progressively increased throughout the culture period (Figure 1C). To further confirm these results, we performed two more replicates of competitive growth of the dCas9-HDAC and HAT pools followed by amplicon sequencing (Table S2). The population of parasite lines in the pools was highly consistent among each replicate with high correlation scores (Figure S3). To statistically assess the changes upon alteration of target gene expression by rapamycin induction, we measured the fold change of each gRNA in the HAT and HDAC pools under normal growth conditions without rapamycin induction. The resulting fold changes across all time points follow a Gaussian distribution with the majority centered around 0 (Figure S4). Based on this normal distribution, we estimated the *p* values of the fold changes after rapamycin induction using maximum likelihood estimation and referred to these comparisons as the "fitness score."

Consistently, the populations of *AP2G*-HAT and *ATG18*-HAT were more than 2-fold and slightly reduced 11 days after induction, respectively (Figure 1D). Surprisingly, upregulation of *DNMT* and *MYST* in *DNMT*-HAT and *MYST*-HAT led to a significant increase of these parasites in the competitive growth condition, whereas downregulation of *AP2G* and *CRT* in *AP2G*-HDAC and *CRT*-HDAC resulted in substantial decreases of these parasites in the pool (Figure 1E). We reflected on why we did not observe these growth phenotypes in the earlier individual parasite culture[31] and noticed that the continuous culture for all individual growth assays was conducted for only two IDCs, unlike competitive growth for six IDCs (Figure 1D). Therefore, we compared the individual growth of four parasite lines (*AP2G*-HAT, *DNMT*-HAT, *AP2G*-HDAC, and *CRT*-HDAC) over a longer period (4 IDCs) and validated the growth phenotypes observed in the competitive growth conditions (Figure S5). Because previous studies suggested that *AP2G* might be involved in the regulation of merozoite invasion,[32,33] we measured the capacity of merozoite invasion and observed a reduction in the invasion rate of *AP2G*-HDAC (Figure S5).

To validate that the observed growth phenotypes in the pooled culture were indeed attributed to the regulation of the target genes, we performed reverse transcriptase and real-time PCR to measure the transcription levels of target genes in the pools at the late trophozoite stage 30 h after rapamycin was added to the pools at the ring stage. All seven tested genes were transcriptionally increased or decreased in the dCas9-HDAC and HAT pools, respectively, after induction (+rap) compared with their uninduced controls (−rap) (Figure S6).

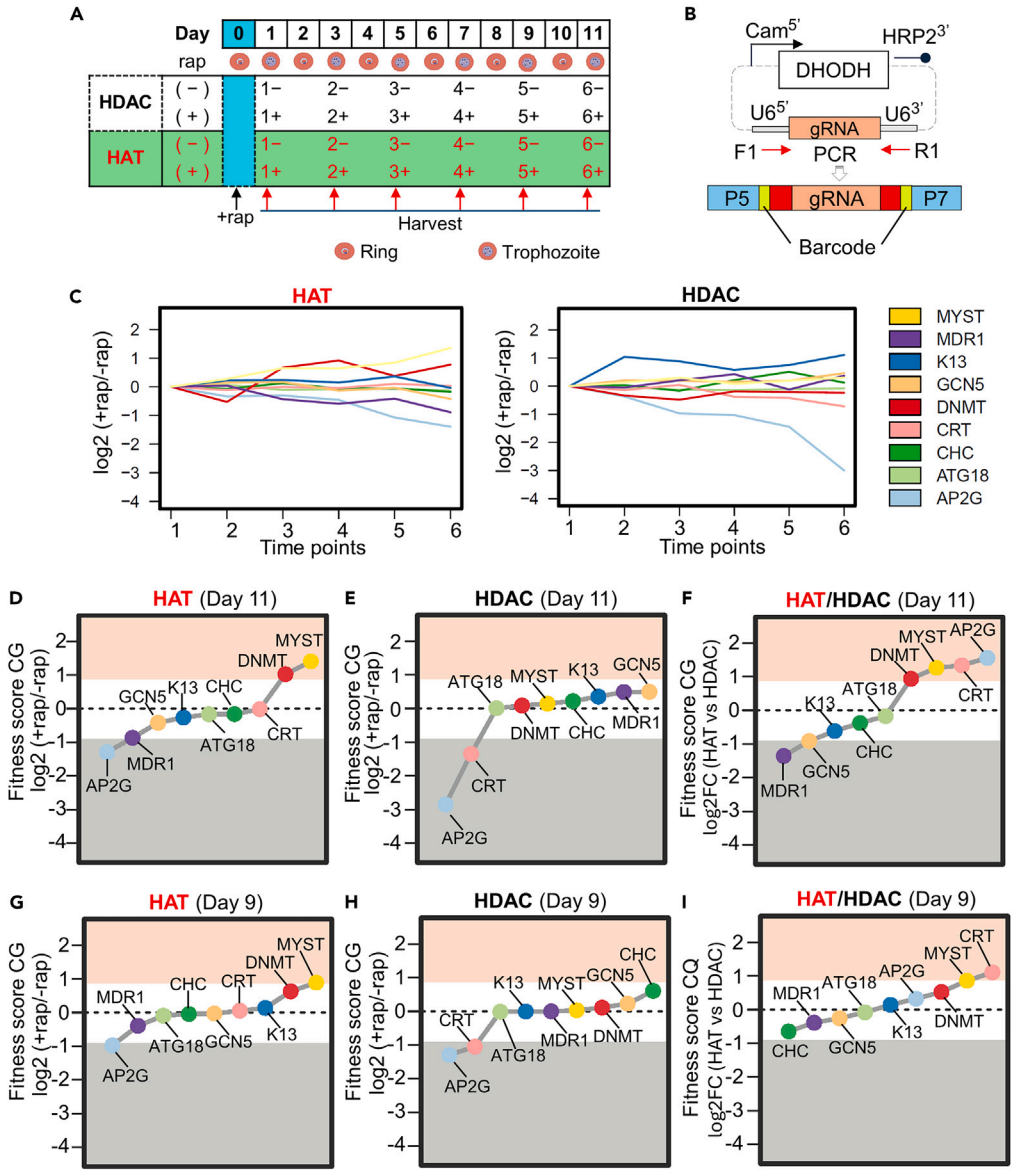

Figure 1. Phenotype screening via CRISPRi/a in competitive growth condition

(A) DNA collection timeline from HDAC (white shade) and HAT (green shade) pools. Ring-stage pools were treated with (+) overnight or without (−) rap induction on day 0. gDNA was harvested at 6 time points denoted by numbers in the table.

(B) Schematic of plasmid and the gRNA locus that was PCR amplified by F1 and R1 primers for multiplexed amplicon sequencing. P5 and P7 denote Illumina adapters for pair-end sequencing. DHODH, dihydroorotate dehydrogenase drug cassette.

(C) Relative abundance of each parasite line in a pool over time after rap induction (+rap) of dCas9-HAT (left) and -HDAC (right) compared with their uninduced control (−rap). The y axis shows log2 fold changes of read counts of +rap compared with −rap. The x axis shows time points.

(D and E) Fitness score under the competitive growth (CG) at day 11 showing log2 fold changes of read counts at the 6th time point from different parasite clones after rapamycin induction of dCas9-HAT (D) and -HDAC (E) modules.

(F) Fitness score under CG at day 11 between HAT and HDAC pools showing the log2 fold changes of gRNAs between dCas9-HAT and -HDAC modules.

(G and H) Fitness score under CG at day 9 showing log2 fold changes of read counts at the 5th time point from different parasite clones after rapamycin induction of dCas9-HAT (G) and -HDAC (H) modules.

(I) Fitness score under CG at day 9 showing the log2 fold changes of gRNAs between dCas9-HAT and -HDAC modules. The red or gray areas in (D–I) denote the statistical significance of the growth advantage or disadvantage, respectively.

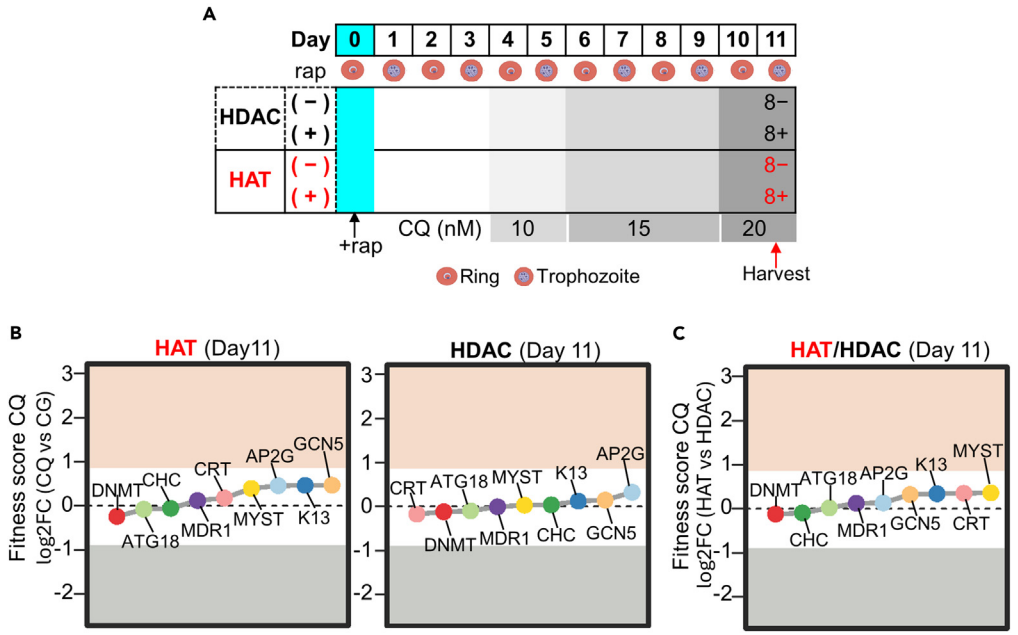

Figure 2. CRISPRi/a screening under chloroquine treatment

(A) DNA collection timeline from dCas9-HDAC and -HAT pools. Ring-stage pools were treated with (+) overnight or without (−) rap induction on day 0. CQ treatment (10 nM) started on day 4. CQ concertation was increased gradually to 15 and 20 nM. DNA was harvested at 8 days post-initial CQ treatment.

(B) Fitness score under CQ treatment showing log2 fold changes (FCs) of gRNAs under CQ treatment normalized by the competitive growth (CG) at day 11 after rapamycin induction.

(C) Fitness score under CQ treatment showing the log2 FCs of gRNAs between dCas9-HAT and -HDAC modules under CQ treatment. The red or gray areas in (B and C) denote the statistical significance of the growth advantage or disadvantage, respectively.

Upregulation of *DNMT* substantially elevated the growth of *DNMT*-HAT (Figure 1D), suggesting this is a fitness-enhancing gene, in agreement with a previous study showing that conditional knockout of *DNMT* rendered mutant parasites more sensitive to cellular stress.[34] Downregulation of *CRT* significantly reduced the growth of *CRT*-HDAC (Figure 1E), indicating this gene is important for parasite growth probably because of its critical physiological role in the export of metabolites out of food vacuole.[35,36] Notably, the growth phenotype of each parasite line in the HAT pool was reversed in the HDAC pool except *AP2G*, indicating that up-and downregulation of target genes caused the opposite effects. This observation aligns with the findings in many CRISPRi/a screens[13,37–39] (Figures 1D and 1E). Directly comparing the parasite populations in the HAT pool with those in the HDAC pool helps us further highlight the pattern of fitness upon up- and downregulation of the target gene (Figure 1F). This comparison reveals that the upregulation of *MYST*, *CRT*, and *AP2G* led to a significant growth advantage over their downregulation, whereas the upregulation of *MDR1* had a substantial negative impact on parasite growth compared with its downregulation. These growth phenotypes at day 11 after induction were also observed at an earlier time point (day 9) but to a lesser extent (Figures 1G–1I). Collectively, our inducible CRISPRi/a screen under competitive growth demonstrated that this genetic screen was sensitive and robust and has the potential to screen a repertoire of genes that are essential for the parasite's survival.

CRISPRi/a screen identifies genes responsive to chloroquine treatment

To explore the adaptability of our screening tool to antimalarial selection strategies, we subjected HDAC and HAT pools to chloroquine (CQ) pressure. We modulated dCas9-HAT and -HDAC expression by exposing pools to rapamycin (+rap) overnight and started adding CQ 4 days later along with parallel controls (−rap). CQ treatment was started at a sub-lethal concentration (10 nM) for two days as the IC_{50} for 3D7 is ~20 nM[40–42] and continuously increased to 15 nM for three days and 20 nM for 2 days without observable cell death (Figure 2A). On the 4th IDC (day 8 post-CQ treatment), the abundance of gRNAs in the pools was measured by amplicon sequencing. We performed two more replicates of screens and once again showed the high reproducibility of these screens (Figure S3). The changes in parasite populations between induction (+rap) and their control (−rap) under CQ pressure were first calculated and further normalized by the competitive growth (CG) shown in Figure 1D to exclude fitness growth factors induced by the competitive growth (Figure 2B).

Overall, no parasite line in the HAT and HDAC pools showed significant changes upon CQ treatment although an opposite trend of growth phenotypes was observed for *CRT*-HAT and *CRT*-HDAC (Figure 2B, Table S2). *P. falciparum CRT* encodes a chloroquine transporter and is the primary determinant of chloroquine resistance.[43] Therefore, it was expected that reducing *CRT* expression would negatively impact *CRT*-HDAC's fitness in the pool, whereas upregulating *CRT* would conversely enhance the fitness of *CRT*-HAT when the parasites are under

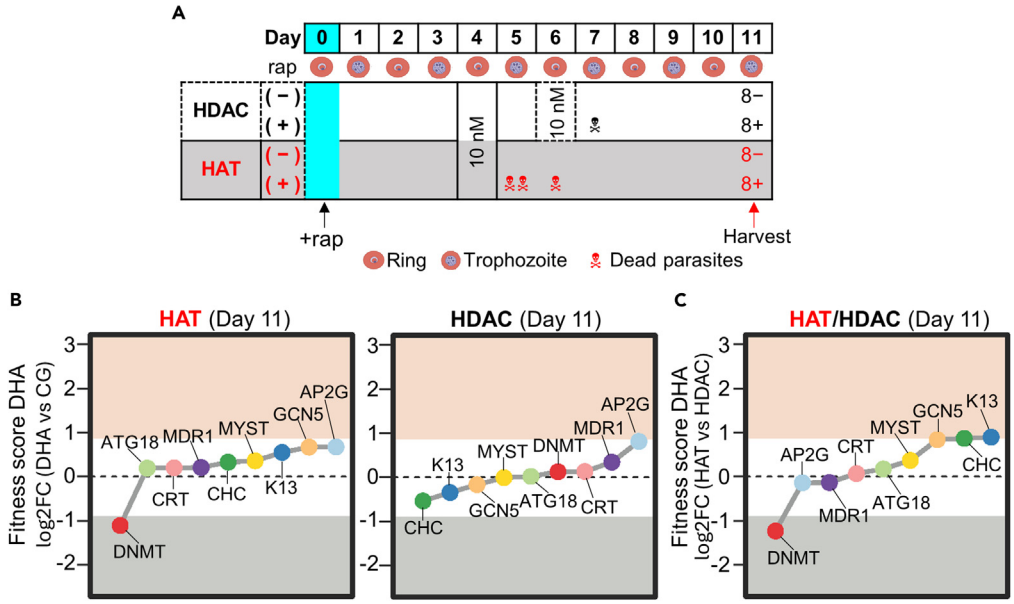

Figure 3. CRISPRi/a screening under DHA treatment

(A) DNA collection timeline from dCas9-HDAC and -HAT pools. Ring-stage pools were treated with (+) overnight or without (–) rap induction on day 0. DHA treatment (10 nM) started on day 4. gDNA of the dCas9-HAT pool was harvested on day 8 post-initial DHA treatment. dCas9-HDAC pool was treated one more time on day 6, and gDNA was harvested at day 6 post-initial DHA treatment. ☠ denotes parasite death.

(B) Fitness score under DHA treatment showing the fold changes (FCs) of gRNAs under DHA treatment normalized by the competitive growth (CG) at day 11 after rapamycin induction.

(C) Fitness score under DHA treatment showing log2 FCs of gRNAs between dCas9-HAT and -HDAC modules under DHA treatment. The red or gray areas in (B and C) denote the statistical significance of the growth advantage or disadvantage, respectively.

CQ pressure. Consistently, *CRT*-HAT and *CRT*-HDAC were slightly increased and decreased (1.13-fold up and down) upon CQ treatment, respectively, indicating that *CRT*-HAT survived better than *CRT*-HDAC under CQ pressure (Figure 2B). This trend was emphasized when the HAT pool was directly compared with the HDAC pool, revealing that *CRT* was the second-best gene for parasite survival upon CQ treatment (Figure 2C, 1.28-fold). Besides *CRT*, upregulation of *K13*, *MYST*, and GCN5 favored the corresponding parasite lines' fitness under treatment (Figures 2B and 2C). *GCN5* and *K13* are known to be involved in stress response,[44–51] and *MYST* is involved in DNA repair,[52] which may explain their impact on the fitness of the parasite under CQ pressure.

CRISPRi/a screen identifies genes responsible for dihydroartemisinin treatment

We further validated our screening tool using a first-line antimalarial, dihydroartemisinin (DHA). After two IDCs of rap-induced gene modulation, we treated the ring-stage pools with DHA for 6 h at 10 nM, which is ~20 x IC_{50}[42,53] (Figure 3A). Interestingly, the parasites from the pooled set of dCas9-HAT showed substantial death on the next day. Eventually, the parasites grew up to a level suitable for harvest 8 days after DHA treatment. Meanwhile, the parasites from the pooled set of dCas9-HDAC did not show immediate death following DHA treatment, thus we repeated the DHA treatment at the subsequent ring stage during the second IDC and observed a low level of parasite death on the following day (Figure 3A). We allowed the parasites to recover and harvested gDNA at the trophozoite stage 5 days after the second DHA treatment. The population of each parasite clone was analyzed after PCR of gRNA loci and amplicon sequencing (Table S2).

The population of *K13*-HDAC decreased to 78%, whereas the growth of *K13*-HAT increased (1.46-fold) upon DHA treatment, indicating that *K13* expression is positively correlated with the parasite fitness under DHA treatment (Figure 3B). This trend was prominent (1.86-fold) when the populations in the HAT pool were compared with those in the HDAC pool (Figure 3C), showing that *K13* was the most significant gene for parasite survival under DHA treatment. These results are consistent with a previous report showing that the mislocalization of K13 from the cytosol to the nucleus (knock sideways) led to an arrest at the ring stage.[54] A recent transcriptomic analysis study showed that *K13* was substantially downregulated (2.77-fold) upon a low dose (30 nM) of DHA treatment at the early ring stage.[51] Thus, a low dose of DHA treatment in this screen may cause downregulation of *K13*, leading to further reduction of *K13* expression levels in *K13*-HDAC. This may eventually make the *K13*-HDAC parasite less fit for growth than *K13*-HAT under DHA.

The same opposite trends were exhibited for *CHC* and *GCN5*, showing improved survival (1.25- and 1.59-fold) in *CHC*-HAT and *GCN5*-HAT and decreased survival in *CHC*-HDAC and *GCN5*-HDAC (31% and 11% reduction), respectively, consistent with previous evidence that *GCN5* genes are associated with artemisinin resistance by playing a role in important pathways such as stress response[44,51,55] (Figures 3B and

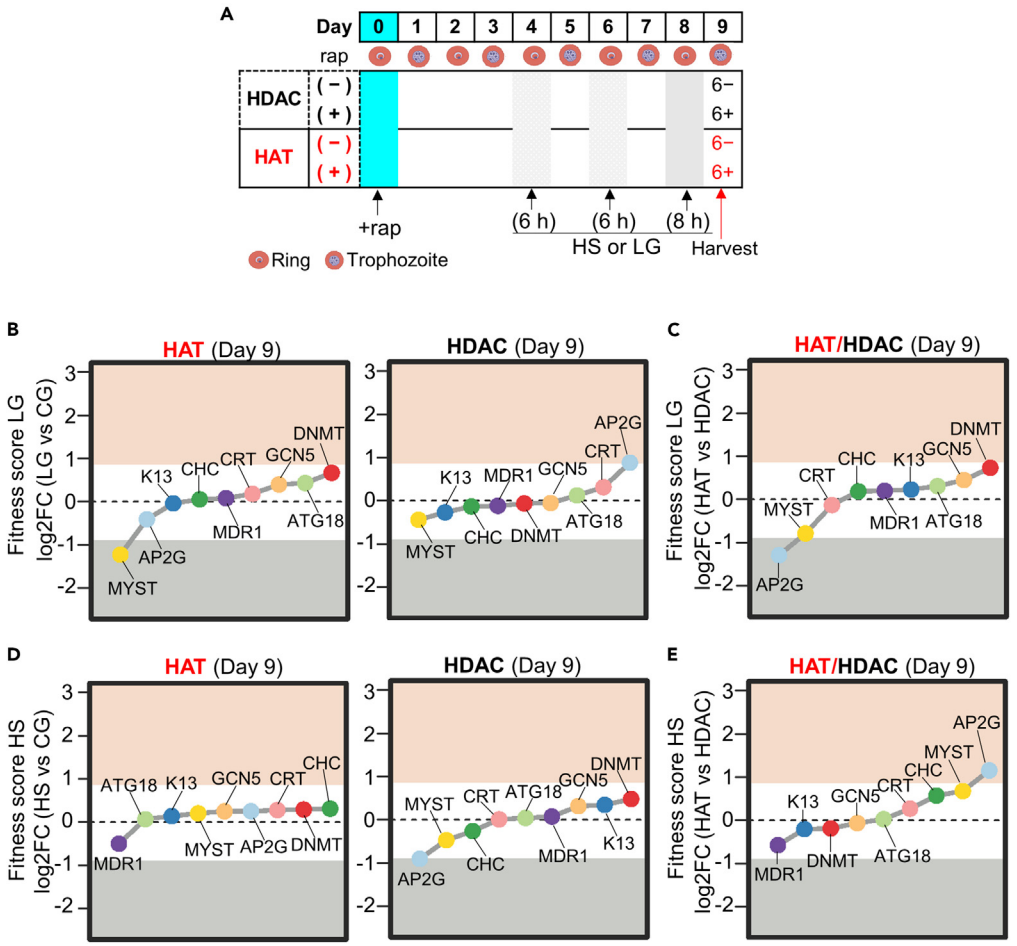

Figure 4. CRISPRi/a screening under LG and HS conditions

(A) DNA collection timeline from dCas9-HDAC and -HAT pools. Ring-stage pools were treated with (+) overnight or without (−) rap induction on day 0. Low-glucose (LG) (0.5 g/L) starvation or HS (41°C) were applied to the ring-stage parasites for 6 h or 8 h on days 4, 6, and 8, respectively. DNA was harvested on day 6 post-initial LG starvation or HS.

(B) Fitness score under LG stress showing the log2 fold changes (FCs) under LG normalized by the competitive growth (CG) at day 9 after three times of LG treatment.

(C) Fitness score under LG stress showing the log2 FCs of gRNAs between dCas9-HAT and -HDAC modules under LG condition.

(D) Fitness score under HS stress showing the log2 FCs of gRNAs under HS normalized by CG at day 9 after three times of HS treatment.

(E) Fitness score under HS stress showing the log2 FCs of gRNAs between dCas9-HAT and -HDAC modules under HS condition. The red or gray areas in (B–E) denote the statistical significance of the growth advantage or disadvantage, respectively.

3C). Conversely, the upregulation of *DNMT* led to significant negative growth of *DNMT*-HAT (54% reduction), whereas its downregulation in *DNMT*-HDAC resulted in slightly increased survival (Figure 3B).

CRISPRi/a screen identifies genes involved in nutritional and heat stress responses

Malaria parasites employ defense mechanisms to survive various stress conditions, including cyclical fever (heat shock, HS), as well as starvation caused by low blood sugar levels (hypoglycemia) within their human hosts.[56,57] To evaluate whether our CRISPRi/a screen can be deployed to identify the repertoire of genes needed by parasites to respond to these stress conditions, we modulated gene expression in the pooled parasite sets via activation of CRISPRi/a by rap (+rap) for 2 IDCs and then applied starvation and HS conditions to the HDAC and HAT pools by using low glucose (LG) (0.5 g/L) medium and 41°C for 6 h at the ring stage of the 3rd and 4th IDC (Figure 4A). The reason we applied stress to the ring-stage parasites is that this stage is the most tolerant stage to starvation and HS compared with other asexual stages.[44,45,51,57–60] At the beginning of the 5th cycle, a third round of stress conditions was applied for 8 h at the ring stage. Consistently, no noticeable growth defects (parasite death) were identified after three repeats of stress conditions were applied. We harvested parasites on the next day after the 8-h stress conditions at the trophozoite stage (day 6 post-initial starvation) for amplicon sequencing (Figure 4A, Table S2).

Similar to the competitive growth screening, upregulation of *DNMT* also caused a positive fitness under LG (Figures 4B, 4C, 1D, and 1F), further validating that *DNMT* is involved in stress response.[34] Up- and downregulation of *GCN5* resulted in higher survival of *GCN5*-HAT (1.32-fold) and a slight decrease of *GCN5*-HDAC under LG (Figures 4B and 4C), consistent with the finding that GCN5 was involved in stress responses to the starvation.[44,45,51] Similar patterns were also displayed for *ATG18*, in agreement with earlier reports that this gene coordinates stress response[61] (Figures 4B and 4C). Interestingly, in LG conditions, both up-and downregulation of *MYST* led to a growth disadvantage (53% reduction) (Figure 4B). Conversely, up-and downregulation of *AP2G* caused a reduction in the HAT pool and a substantial growth advantage (1.84-fold) in the HDAC pool, respectively (Figure 4B). It is well known that stress, especially starvation, can induce gametocytogenesis, and our previous report showed that upregulation of *AP2G* in HAT-*AP2G* led to higher gametocytogenesis under normal growth conditions.[31,62] Thus, LG could induce gametocytogenesis of HAT-*AP2G* at even higher levels and reduce its asexual population to a larger extent compared with the normal growth condition.

The patterns of parasite fitness under HS were in general different from the ones under LG except that upregulation of *GCN5* and *DNMT* also conferred better growth fitness (Figures 4D and 4E). In contrast, the downregulation of *GCN5* and *DNMT* also exhibited growth advantages, whereas the alteration of *AP2G* caused the opposite growth pattern compared with those under LG (Figures 4B–4E). Additionally, up- and downregulation of *MYST* resulted in better and worse growth fitness, respectively, linking the function of *PfMYST* in DNA repair and DNA fragmentation to heat exposure.[52,57,58] These results are consistent with our recent transcriptomic analysis showing that two different stress conditions led to both common and stress-specific responses.[51]

Generation of screen libraries by single transfection of mixed plasmids

To simplify the approach to the generation of screening libraries, we ought to investigate whether the plasmids expressing different gRNAs could be introduced into dCas9-HAT and dCas9-HDAC parasite lines by a single transfection. First, we performed transfection with a mixture of equal amounts of 10 plasmids expressing 10 gRNA targeting 5 autophagy-related genes (Table S1). After the parasites appeared under WR99210 selection, they were harvested for amplicon sequencing. Sequencing reads corresponding to all 10 gRNAs were identified from the transfected parasites (Figure 5A, Table S2). We then conducted two replicates of transfection into both dCas9-HAT and dCas9-HDAC parasite lines with a mixture of 41 plasmids expressing 41 gRNAs targeting 21 genes (Table S1). Amplicon sequencing identified all gRNAs in all replicates (Figures 5B, 5C, S7A, and S7B; Table S2). Interestingly, the distribution of each gRNA in the pools was different in each transfection, indicating the populations of parasites containing each gRNA were not equal in the pools. We found that if we equally mix parasite cultures from two transfections, the populations of parasites expressing different gRNAs in the new mixed pools will be relatively evenly distributed (Figures 5D and S7C).

DISCUSSION

To investigate whether the conditional CRISPRi/a system can be used for genetic screening in *P. falciparum*, here we conducted a series of small-scale screenings by using two sets of pools consisting of nine single parasite lines, each carrying an individual gRNA targeting the respective nine genes in catalytically deadCas9 (dCas9)-fused repressive (HDAC) or activating (HAT) parasite backgrounds.[31] The dCas9-HAT and -HDAC pools were screened under five different conditions: competitive growth, CQ and DHA treatments, and HS and LG starvation conditions. By using the same approach in a recent study of a small-scale screen in *leishmania*,[25] the population of each parasite line in the pool was measured by calculating the reads number of specific gRNAs from the amplicon sequencing. By analyzing these screens, we demonstrated that this system is simple and robust for forward genetic screening in *P. falciparum*.

Several aspects of our detailed analysis demonstrated these screens were successful and sensitive. First, in the competitive growth screen, *AP2G*-HAT and *ATG18*-HAT showed negative growth in the pools, respectively, consistent with the previous finding that individual upregulation of *AP2G* and *ATG18* by two different gRNA-3 led to high gametocytogenesis and a growth defect, respectively[31] (Figure 1D). Furthermore, our long-term culture of 4 individual parasite lines (*AP2G*-HDAC, *AP2G*-HAT, *DNMT*-HAT, and *CRT*-HAT) validated the growth phenotypes in the competitive growth (Figures 1D and S5). Second, in the screens by CQ treatment, the populations of *CRT*-HDAC and *CRT*-HAT were reduced and increased, respectively, congruent with the findings that *PfCRT* is the primary determinant of CQ resistance[43] (Figure 2). Third, in the screens under DHA treatment, upregulation of *K13* and *GCN5* induced a growth advantage during DHA stress, consistent with the discovery that K13 is involved in the response to DHA and GCN5 positively mediated stress response under DHA treatment.[44,51,54] Fourth, the upregulation of *GCN5* resulted in a growth advantage in both HS and LG starvation screens, in agreement with a recent study showing that GCN5 positively mediated stress response under HS and LG conditions.[51]

K13 data from our screens under DHA treatment do not agree with the previous reports that showed that up- and downregulation of *K13* rendered parasites more and less sensitive to DHA treatment in the recovery assay (RA), respectively.[31] Additionally, lower expression of K13 increased the resistance to ART by the ring-stage survival assay (RSA).[63–65] The discrepancy in the abovementioned results is likely because the concentration (10 nM) of DHA we used in this study is much lower than the ones used in RA (1 mM) and RSA (700 nM).

Besides the abovementioned reasonable outcomes, we also noted some unexpected results. In the screen of competitive growth, the downregulation of *AP2G* resulted in a growth disadvantage in the pools due to the reduced capacity of invasion (Figures 1 and S5). These results were unexpected because *AP2G* is widely recognized as a master regulator of gametocytogenesis rather than asexual growth.[32,33,66,67] However, a previous study found that AP2G potentially regulates invasion genes by its occupancy to the promoters of invasion genes and its interaction with AP2-I, a transcription factor regulating merozoite invasion.[32] Additionally, transcriptomic analysis by microarray showed that

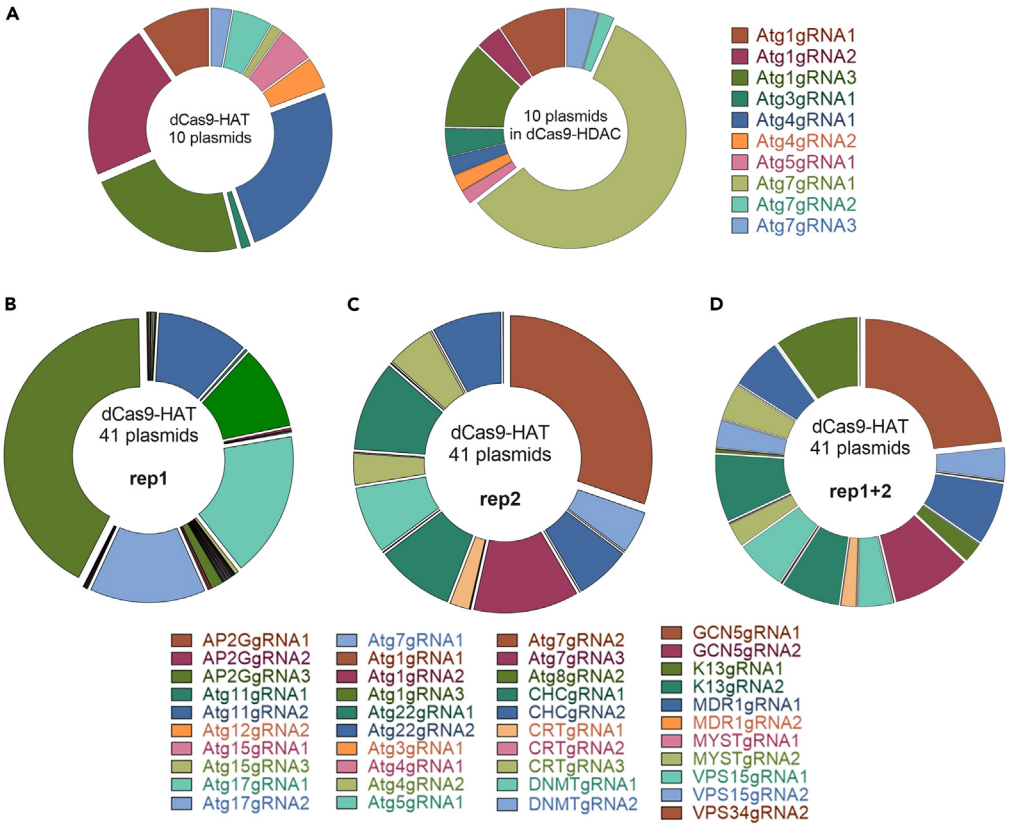

Figure 5. The generation of screening libraries by single transfection

(A) Proportions of each plasmid in the parasites after transfection of a mixture of 10 plasmids expressing 10 different gRNAs into dCas9-HAT or dCas9-HDAC parasite line.

(B and C) Pie charts show the distributions of 41 gRNAs in the parasite culture after a mixture of 41 plasmids was introduced into dCas9-HDAC by two replicates (rep1 and rep2) of transfections.

(D) Pie chart shows the distribution of 41 gRNAs in the parasite culture if the two transfected cultures are equally mixed (rep1+rep2).

AP2-G KO caused downregulation of one invasion-related gene (CLAG2, PF3D7_0220800) by using criteria of >2-fold.[33] These findings collectively suggest that *AP2G* has additional functions in asexual development beyond its recognized role in gametocytogenesis.

We observed that even before rap induction in the normal cultured pools, the population of each parasite line gradually altered, suggesting that unknown forces drove these changes; this could be attributed to the transient binding of two elements of DiCre causing the activation of dCas9-HDAC or -HAT in some parasites, which might randomly silence or activate targeting genes at low frequency. Upon rap induction, the parasite population experienced much larger rates of alteration, facilitating the feasibility of these screens (Figure S2).

A major advantage of our screen system is that it activates or represses gene expression simply by introducing specific gRNA without scarring the genome; therefore, essential genes can be studied by this system. Moreover, our screen system achieves opposite directions of gene control (activation and repression), which provides reciprocal evidence of the genetic screen and gene functions. Despite the abovementioned advantages, we also observed that some changes in the screens did not reach statistical significance. For example, *CRT* under the CQ treatment was rated as the top gene for parasite survival and was near the statistically significant level (Figures 2, 3, and 4). These results were probably because some up- or downregulations by dCas9-HAT or -HDAC were not strong enough. Several approaches could address this limitation. First, maximizing the number of gRNAs for each gene will enhance the potential for effective gene regulation. This approach has been widely used in the published CRISPRi or CRISPRa screens. Second, a direct comparison of the complementary results from parallel screens with CRISPRi and CRISPRa targeting the same gene with the same gRNA will enhance the signal to identify the hits. Our data (Figures 1, 2, 3, and 4) in this manuscript showed that the opposite phenotype upon up- and downregulation of the same gene commonly occurred in CRISPRi and CRISPRa screens.[13,37–39] Third, as the results show in the competitive growth (Figure 1), the changes in the gRNA population gradually increased throughout the culture. Additional rounds of screens may lead to larger variation and eventually result in statistical significance. Fourth, instead of dCas9 that requires "NGG" as Protospacer Adjacent Motif (PAM) for gRNA selection, dCas12a can be used in the conditional CRISPRi/a system because dCas12a uses "TTTN" as PAM. This T-rich PAM provides a significantly higher number of gRNAs in the 5′ UTRs of *P. falciparum* genes. Our preliminary data show that dCas12a works well in CRISPRi/a system.

The mixed plasmids expressing different gRNAs were successfully introduced into parasites by single transfection (Figure 5). This approach will greatly simplify the generation of a screening library and allow us to easily generate libraries targeting different pathways such as invasion or functional categories such as transporters. In summary, our findings highlight the potential of a CRISPRi/a system to screen essential genes in *P. falciparum*, which will greatly facilitate the time-consuming study of gene functions and will provide new insights into developing effective antimalarial therapies.

Limitations of the study

One potential caveat of this screening system is that it is difficult to select suitable gRNAs for certain genes because of the AT-rich nature of genomic DNA in *Plasmodium falciparum*, which limits the selection of gRNA due to the limited number of NGG, the PAM for dCas9,[68] in the promoter of certain genes. This limitation can be overcome by using multiple gRNAs to target a single gene or using dCas12 instead of dCas9 because previous studies showed multiple gRNAs targeting a single gene's promoter can exert significant synergistic regulation effects to substantially strengthen dCas9-based transcriptional activation and repression, and the PAM for Cas12a is T-rich (TTTV; V can be C, G, or A).[31,69–74]

STAR★METHODS

Detailed methods are provided in the online version of this paper and include the following:

- KEY RESOURCES TABLE
- RESOURCE AVAILABILITY
  - Lead contact
  - Materials availability
  - Data and code availability
- EXPERIMENTAL MODEL AND STUDY PARTICIPANT DETAILS
- METHOD DETAILS
  - Parasite culture and invasion assays
  - Generation of parasite lines regulating MDR1 and RT-PCR
  - Pooling clones for mixed cultivation
  - Chloroquine treatment
  - DHA treatment
  - Low glucose starvation
  - Heat stress
  - Transfection of mixed plasmids
  - Amplicon sequencing
  - Amplicon-seq analysis
- QUANTIFICATION AND STATISTICAL ANALYSIS

SUPPLEMENTAL INFORMATION

Supplemental information can be found online at https://doi.org/10.1016/j.isci.2024.109602.

ACKNOWLEDGMENTS

This study was supported by the startup fund from Morsani College of Medicine, University of South Florida and grant R21AI149202 from the National Institute of Allergy and Infectious Diseases (NIAID), NIH, USA to J.M. We thank the University of South Florida Genomics Program (Sequencing Core and Computational Core/Omics Hub) for supporting NGS sequence and data analysis.

AUTHOR CONTRIBUTIONS

J.M. conceived and designed the study. A.B.L. performed research and acquired data. C.W. analyzed amplicon-seq data. A.M. generated plasmids for transfection of mixed plasmids. X.L. generated and analyzed *MDR1*-based dCas9-HAT/HDAC. X.Li. conducted parasite culture and transfection. A.B.L. wrote the original draft. A.B.L. and J.M. revised the manuscript.

DECLARATION OF INTERESTS

The authors declare no competing interests.

Received: August 9, 2023
Revised: February 11, 2024
Accepted: March 25, 2024
Published: March 27, 2024

REFERENCES

1. WHO (2023). World Malaria Report 2023. Geneva (WHO).
2. WHO (2021). Full Evidence Report on the RTS,S/AS01 Malaria Vaccine (SAGE Yellow B).
3. Stokes, B.H., Ward, K.E., and Fidock, D.A. (2022). Evidence of Artemisinin-Resistant Malaria in Africa. N. Engl. J. Med. *386*, 1385–1386. https://doi.org/10.1056/NEJMc2117480.
4. Ashley, E.A., Dhorda, M., Fairhurst, R.M., Amaratunga, C., Lim, P., Suon, S., Sreng, S., Anderson, J.M., Mao, S., Sam, B., et al. (2014). Spread of artemisinin resistance in Plasmodium falciparum malaria. N. Engl. J. Med. *371*, 411–423. https://doi.org/10.1056/NEJMoa1314981.
5. Dhorda, M., Amaratunga, C., and Dondorp, A.M. (2021). Artemisinin and multidrug-resistant Plasmodium falciparum - a threat for malaria control and elimination. Curr. Opin. Infect. Dis. *34*, 432–439. https://doi.org/10.1097/QCO.0000000000000766.
6. van der Pluijm, R.W., Imwong, M., Chau, N.H., Hoa, N.T., Thuy-Nhien, N.T., Thanh, N.V., Jittamala, P., Hanboonkunupakarn, B., Chutasmit, K., Saelow, C., et al. (2019). Determinants of dihydroartemisinin-piperaquine treatment failure in Plasmodium falciparum malaria in Cambodia, Thailand, and Vietnam: a prospective clinical, pharmacological, and genetic study. Lancet Infect. Dis. *19*, 952–961. https://doi.org/10.1016/S1473-3099(19)30391-3.
7. Yeh, E., and DeRisi, J.L. (2011). Chemical rescue of malaria parasites lacking an apicoplast defines organelle function in blood-stage Plasmodium falciparum. PLoS Biol. *9*, e1001138. https://doi.org/10.1371/journal.pbio.1001138.
8. Zhang, M., Wang, C., Otto, T.D., Oberstaller, J., Liao, X., Adapa, S.R., Udenze, K., Bronner, I.F., Casandra, D., Mayho, M., et al. (2018). Uncovering the essential genes of the human malaria parasite Plasmodium falciparum by saturation mutagenesis. Science *360*, eaap7847. https://doi.org/10.1126/science.aap7847.
9. Wang, T., Birsoy, K., Hughes, N.W., Krupczak, K.M., Post, Y., Wei, J.J., Lander, E.S., and Sabatini, D.M. (2015). Identification and characterization of essential genes in the human genome. Science *350*, 1096–1101. https://doi.org/10.1126/science.aac7041.
10. Koike-Yusa, H., Li, Y., Tan, E.P., Velasco-Herrera, M.D.C., and Yusa, K. (2014). Genome-wide recessive genetic screening in mammalian cells with a lentiviral CRISPR-guide RNA library. Nat. Biotechnol. *32*, 267–273. https://doi.org/10.1038/nbt.2800.
11. Shalem, O., Sanjana, N.E., Hartenian, E., Shi, X., Scott, D.A., Mikkelson, T., Heckl, D., Ebert, B.L., Root, D.E., Doench, J.G., and Zhang, F. (2014). Genome-Scale CRISPR-Cas9 Knockout Screening in Human Cells. Science *343*, 84–87. https://doi.org/10.1126/science.1247005.
12. Peters, J.M., Colavin, A., Shi, H., Czarny, T.L., Larson, M.H., Wong, S., Hawkins, J.S., Lu, C.H.S., Koo, B.M., Marta, E., et al. (2016). A Comprehensive, CRISPR-based Functional Analysis of Essential Genes in Bacteria. Cell *165*, 1493–1506. https://doi.org/10.1016/j.cell.2016.05.003.
13. Gilbert, L.A., Horlbeck, M.A., Adamson, B., Villalta, J.E., Chen, Y., Whitehead, E.H., Guimaraes, C., Panning, B., Ploegh, H.L., Bassik, M.C., et al. (2014). Genome-Scale CRISPR-Mediated Control of Gene Repression and Activation. Cell *159*, 647–661. https://doi.org/10.1016/j.cell.2014.09.029.
14. Bock, C., Datlinger, P., Chardon, F., Coelho, M.A., Dong, M.B., Lawson, K.A., Lu, T., Maroc, L., Norman, T.M., Song, B., et al. (2022). High-content CRISPR screening. Nat. Rev. Methods Primers *2*, 9. https://doi.org/10.1038/s43586-022-00098-7.
15. Cai, R., Lv, R., Shi, X., Yang, G., and Jin, J. (2023). CRISPR/dCas9 Tools: Epigenetic Mechanism and Application in Gene Transcriptional Regulation. Int. J. Mol. Sci. *24*, 14865. https://doi.org/10.3390/ijms241914865.
16. Sidik, S.M., Huet, D., Ganesan, S.M., Huynh, M.H., Wang, T., Nasamu, A.S., Thiru, P., Saeij, J.P.J., Carruthers, V.B., Niles, J.C., and Lourido, S. (2016). A Genome-wide CRISPR Screen in Toxoplasma Identifies Essential Apicomplexan Genes. Cell *166*, 1423–1435.e12. https://doi.org/10.1016/j.cell.2016.08.019.
17. Young, J., Dominicus, C., Wagener, J., Butterworth, S., Ye, X., Kelly, G., Ordan, M., Saunders, B., Instrell, R., Howell, M., et al. (2019). A CRISPR platform for targeted in vivo screens identifies Toxoplasma gondii virulence factors in mice. Nat. Commun. *10*, 3963. https://doi.org/10.1038/s41467-019-11855-w.
18. Bryant, J.M., Baumgarten, S., Glover, L., Hutchinson, S., and Rachidi, N. (2019). CRISPR in Parasitology: Not Exactly Cut and Dried. Trends Parasitol. *35*, 409–422. https://doi.org/10.1016/j.pt.2019.03.004.
19. Sangaré, L.O., Ólafsson, E.B., Wang, Y., Yang, N., Julien, L., Camejo, A., Pesavento, P., Sidik, S.M., Lourido, S., Barragan, A., and Saeij, J.P.J. (2019). In Vivo CRISPR Screen Identifies TgWIP as a Toxoplasma Modulator of Dendritic Cell Migration. Cell Host Microbe *26*, 478–492.e8. https://doi.org/10.1016/j.chom.2019.09.008.
20. Wang, Y.F., Sangare, L.O., Paredes-Santos, T.C., Hassan, M.A., Krishnamurthy, S., Furuta, A.M., Markus, B.M., Lourido, S., and Saeij, J.P.J. (2020). Genome-wide screens identify Toxoplasma gondii determinants of parasite fitness in IFN gamma-activated murine macrophages. Nat. Commun. *11*. https://doi.org/10.1038/s41467-020-18991-8.
21. Waldman, B.S., Schwarz, D., Wadsworth, M.H., 2nd, Saeij, J.P., Shalek, A.K., and Lourido, S. (2020). Identification of a Master Regulator of Differentiation in Toxoplasma. Cell *180*, 359–372.e16. https://doi.org/10.1016/j.cell.2019.12.013.
22. Harding, C.R., Sidik, S.M., Petrova, B., Gnädig, N.F., Okombo, J., Herneisen, A.L., Ward, K.E., Markus, B.M., Boydston, E.A., Fidock, D.A., and Lourido, S. (2020). Genetic screens reveal a central role for heme metabolism in artemisinin susceptibility. Nat. Commun. *11*, 4813. https://doi.org/10.1038/s41467-020-18624-0.
23. Li, W., Grech, J., Stortz, J.F., Gow, M., Periz, J., Meissner, M., and Jimenez-Ruiz, E. (2022). A splitCas9 phenotypic screen in Toxoplasma gondii identifies proteins involved in host cell egress and invasion. Nat. Microbiol. *7*, 882–895. https://doi.org/10.1038/s41564-022-01114-y.
24. Smith, T.A., Lopez-Perez, G.S., Herneisen, A.L., Shortt, E., and Lourido, S. (2022). Screening the Toxoplasma kinome with high-throughput tagging identifies a regulator of invasion and egress. Nat. Microbiol. *7*, 868–881. https://doi.org/10.1038/s41564-022-01104-0.
25. Engstler, M., and Beneke, T. (2023). Gene editing and scalable functional genomic screening in Leishmania species using the CRISPR/Cas9 cytosine base editor toolbox LeishBASEedit. Elife *12*, e85605. https://doi.org/10.7554/eLife.85605.
26. Walker, M.P., and Lindner, S.E. (2019). Ribozyme-mediated, multiplex CRISPR gene editing and CRISPR interference (CRISPRi) in rodent-infectious Plasmodium yoelii. J. Biol. Chem. *294*, 9555–9566. https://doi.org/10.1074/jbc.RA118.007121.
27. Bushell, E., Gomes, A.R., Sanderson, T., Anar, B., Girling, G., Herd, C., Metcalf, T., Modrzynska, K., Schwach, F., Martin, R.E., et al. (2017). Functional Profiling of a Plasmodium Genome Reveals an Abundance of Essential Genes. Cell *170*, 260–272.e8. https://doi.org/10.1016/j.cell.2017.06.030.
28. Oberstaller, J., Otto, T.D., Rayner, J.C., and Adams, J.H. (2021). Essential Genes of the Parasitic Apicomplexa. Trends Parasitol. *37*, 304–316. https://doi.org/10.1016/j.pt.2020.11.007.
29. Kimmel, J., Schmitt, M., Sinner, A., Jansen, P.W.T.C., Mainye, S., Ramón-Zamorano, G., Toenhake, C.G., Wichers-Misterek, J.S., Cronshagen, J., Sabitzki, R., et al. (2023). Gene-by-gene screen of the unknown proteins encoded on Plasmodium falciparum chromosome 3. Cell Syst. *14*, 9–23.e7. https://doi.org/10.1016/j.cels.2022.12.001.
30. Xu, R., Liu, Y., Fan, R., Liang, R., Yue, L., Liu, S., Su, X.Z., and Li, J. (2019). Generation and functional characterisation of Plasmodium yoelii csp deletion mutants using a microhomology-based CRISPR/Cas9 method. Int. J. Parasitol. *49*, 705–714. https://doi.org/10.1016/j.ijpara.2019.04.003.
31. Liang, X., Boonhok, R., Siddiqui, F.A., Xiao, B., Li, X., Qin, J., Min, H., Jiang, L., Cui, L., and Miao, J. (2022). A Leak-Free Inducible CRISPRi/a System for Gene Functional Studies in Plasmodium falciparum. Microbiol. Spectr. *10*, e0278221. https://doi.org/10.1128/spectrum.02782-21.
32. Josling, G.A., Russell, T.J., Venezia, J., Orchard, L., van Biljon, R., Painter, H.J., and Llinás, M. (2020). Dissecting the role of PfAP2-G in malaria gametocytogenesis. Nat. Commun. *11*, 1503. https://doi.org/10.1038/s41467-020-15026-0.
33. Kafsack, B.F.C., Rovira-Graells, N., Clark, T.G., Bancells, C., Crowley, V.M., Campino, S.G., Williams, A.E., Drought, L.G., Kwiatkowski, D.P., Baker, D.A., et al. (2014). A transcriptional switch underlies commitment to sexual development in malaria parasites. Nature *507*, 248–252. https://doi.org/10.1038/nature12920.
34. Hammam, E., Sinha, A., Baumgarten, S., Nardella, F., Liang, J., Miled, S., Bonhomme, F., Erdmann, D., Arcangioli, B., Arimondo, P.B., et al. (2021). Malaria Parasite Stress Tolerance Is Regulated by DNMT2-Mediated tRNA Cytosine Methylation. mBio *12*, e0255821. https://doi.org/10.1128/mBio.02558-21.
35. Sanchez, C.P., Manson, E.D.T., Cubel, S.M., Mandel, L., Weidt, S.K., Barrett, M.P., and Lanzer, M. (2022). The Knock-Down of the Chloroquine Resistance Transporter PfCRT Is Linked to Oligopeptide Handling in.

Microbiol. Spectr. *10*, e0110122. https://doi.org/10.1128/spectrum.01101-22.
36. Juge, N., Moriyama, S., Miyaji, T., Kawakami, M., Iwai, H., Fukui, T., Nelson, N., Omote, H., and Moriyama, Y. (2015). chloroquine resistance transporter is a H+-coupled polyspecific nutrient and drug exporter. Proc. Natl. Acad. Sci. USA *112*, 3356–3361. https://doi.org/10.1073/pnas.1417102112.
37. Klann, T.S., Black, J.B., Chellappan, M., Safi, A., Song, L., Hilton, I.B., Crawford, G.E., Reddy, T.E., and Gersbach, C.A. (2017). CRISPR-Cas9 epigenome editing enables high-throughput screening for functional regulatory elements in the human genome. Nat. Biotechnol. *35*, 561–568. https://doi.org/10.1038/nbt.3853.
38. Kabadi, A.M., Machlin, L., Dalal, N., Lee, R.E., McDowell, I., Shah, N.N., Drowley, L., Randell, S.H., and Reddy, T.E. (2022). Epigenome editing of the CFTR-locus for treatment of cystic fibrosis. J. Cyst. Fibros. *21*, 164–171. https://doi.org/10.1016/j.jcf.2021.04.008.
39. Jost, M., Chen, Y., Gilbert, L.A., Horlbeck, M.A., Krenning, L., Menchon, G., Rai, A., Cho, M.Y., Stern, J.J., Prota, A.E., et al. (2017). Combined CRISPRi/a-Based Chemical Genetic Screens Reveal that Rigosertib Is a Microtubule-Destabilizing Agent. Mol. Cell *68*, 210–223.e6. https://doi.org/10.1016/j.molcel.2017.09.012.
40. Reiling, S.J., and Rohrbach, P. (2019). Uptake of a fluorescently tagged chloroquine analogue is reduced in CQ-resistant compared to CQ-sensitive Plasmodium falciparum parasites. Malar. J. *18*, 342. https://doi.org/10.1186/s12936-019-2980-y.
41. Edaye, S., Tazoo, D., Bohle, D.S., and Georges, E. (2015). 3-Halo Chloroquine Derivatives Overcome Plasmodium falciparum Chloroquine Resistance Transporter-Mediated Drug Resistance in P. falciparum. Antimicrob. Agents Chemother. *59*, 7891–7893. https://doi.org/10.1128/AAC.01139-15.
42. Zhao, W., Li, X., Yang, Q., Zhou, L., Duan, M., Pan, M., Qin, Y., Li, X., Wang, X., Zeng, W., et al. (2022). In vitro susceptibility profile of Plasmodium falciparum clinical isolates from Ghana to antimalarial drugs and polymorphisms in resistance markers. Front. Cell. Infect. Microbiol. *12*, 1015957. https://doi.org/10.3389/fcimb.2022.1015957.
43. Sidhu, A.B.S., Verdier-Pinard, D., and Fidock, D.A. (2002). Chloroquine resistance in Plasmodium falciparum malaria parasites conferred by pfcrt mutations. Science *298*, 210–213. https://doi.org/10.1126/science.1074045.
44. Rawat, M., Kanyal, A., Sahasrabudhe, A., Vembar, S.S., Lopez-Rubio, J.J., and Karmodiya, K. (2021). Histone acetyltransferase PfGCN5 regulates stress responsive and artemisinin resistance related genes in Plasmodium falciparum. Sci. Rep. *11*, 852. https://doi.org/10.1038/s41598-020-79539-w.
45. Rawat, M., Malhotra, R., Shintre, S., Pani, S., and Karmodiya, K. (2020). Role of PfGCN5 in nutrient sensing and transcriptional regulation in Plasmodium falciparum. J. Bio. Sci. *45*, 11.
46. Mok, S., Stokes, B.H., Gnädig, N.F., Ross, L.S., Yeo, T., Amaratunga, C., Allman, E., Solyakov, L., Bottrill, A.R., Tripathi, J., et al. (2021). Artemisinin-resistant K13 mutations rewire Plasmodium falciparum's intra-erythrocytic metabolic program to enhance survival. Nat. Commun. *12*, 530. https://doi.org/10.1038/s41467-020-20805-w.
47. Mok, S., Ashley, E.A., Ferreira, P.E., Zhu, L., Lin, Z., Yeo, T., Chotivanich, K., Imwong, M., Pukrittayakamee, S., Dhorda, M., et al. (2015). Population transcriptomics of human malaria parasites reveals the mechanism of artemisinin resistance. Science *347*, 431–435. https://doi.org/10.1126/science.1260403.
48. Bridgford, J.L., Xie, S.C., Cobbold, S.A., Pasaje, C.F.A., Herrmann, S., Yang, T., Gillett, D.L., Dick, L.R., Ralph, S.A., Dogovski, C., et al. (2018). Artemisinin kills malaria parasites by damaging proteins and inhibiting the proteasome. Nat. Commun. *9*, 3801. https://doi.org/10.1038/s41467-018-06221-1.
49. Rocamora, F., Zhu, L., Liong, K.Y., Dondorp, A., Miotto, O., Mok, S., and Bozdech, Z. (2018). Oxidative stress and protein damage responses mediate artemisinin resistance in malaria parasites. PLoS Pathog. *14*, e1006930. https://doi.org/10.1371/journal.ppat.1006930.
50. Cui, L., Wang, Z., Miao, J., Miao, M., Chandra, R., Jiang, H., Su, X.Z., and Cui, L. (2012). Mechanisms of in vitro resistance to dihydroartemisinin in Plasmodium falciparum. Mol. Microbiol. *86*, 111–128. https://doi.org/10.1111/j.1365-2958.2012.08180.x.
51. Lucky, A.B., Wang, C., Shakri, A.R., Kalamuddin, M., Chim-Ong, A., Li, X., and Miao, J. (2023). Plasmodium falciparum GCN5 plays a key role in regulating artemisinin resistance-related stress responses. Antimicrob. Agents Chemother. *67*, e0057723. https://doi.org/10.1128/aac.00577-23.
52. Miao, J., Fan, Q., Cui, L., Li, X., Wang, H., Ning, G., Reese, J.C., and Cui, L. (2010). The MYST family histone acetyltransferase regulates gene expression and cell cycle in malaria parasite Plasmodium falciparum. Mol. Microbiol. *78*, 883–902. https://doi.org/10.1111/j.1365-2958.2010.07371.x.
53. Agarwal, P., Anvikar, A.R., Pillai, C.R., and Srivastava, K. (2017). In vitro susceptibility of Indian Plasmodium falciparum isolates to different antimalarial drugs & antibiotics. Indian J. Med. Res. *146*, 622–628. https://doi.org/10.4103/ijmr.IJMR_1688_15.
54. Birnbaum, J., Flemming, S., Reichard, N., Soares, A.B., Mesén-Ramírez, P., Jonscher, E., Bergmann, B., and Spielmann, T. (2017). A genetic system to study Plasmodium falciparum protein function. Nat. Methods *14*, 450–456. https://doi.org/10.1038/nmeth.4223.
55. Miotto, O., Amato, R., Ashley, E.A., MacInnis, B., Almagro-Garcia, J., Amaratunga, C., Lim, P., Mead, D., Oyola, S.O., Dhorda, M., et al. (2015). Genetic architecture of artemisinin-resistant Plasmodium falciparum. Nat. Genet. *47*, 226–234. https://doi.org/10.1038/ng.3189.
56. Thien, H.V., Kager, P.A., and Sauerwein, H.P. (2006). Hypoglycemia in falciparum malaria: is fasting an unrecognized and insufficiently emphasized risk factor? Trends Parasitol. *22*, 410–415. https://doi.org/10.1016/j.pt.2006.06.014.
57. Engelbrecht, D., and Coetzer, T.L. (2013). Turning up the heat: heat stress induces markers of programmed cell death in Plasmodium falciparum in vitro. Cell Death Dis. *4*, e971. https://doi.org/10.1038/cddis.2013.505.
58. Oakley, M.S.M., Kumar, S., Anantharaman, V., Zheng, H., Mahajan, B., Haynes, J.D., Moch, J.K., Fairhurst, R., McCutchan, T.F., and Aravind, L. (2007). Molecular factors and biochemical pathways induced by febrile temperature in intraerythrocytic Plasmodium falciparum parasites. Infect. Immun. *75*, 2012–2025. https://doi.org/10.1128/iai.01236-06.
59. Zhang, M., Wang, C., Oberstaller, J., Thomas, P., Otto, T.D., Casandra, D., Boyapalle, S., Adapa, S.R., Xu, S., Button-Simons, K., et al. (2021). The apicoplast link to fever-survival and artemisinin-resistance in the malaria parasite. Nat. Commun. *12*, 4563. https://doi.org/10.1038/s41467-021-24814-1.
60. Jensen, M.D., Conley, M., and Helstowski, L.D. (1983). Culture of Plasmodium falciparum: the role of pH, glucose, and lactate. J. Parasitol. *69*, 1060–1067.
61. Agrawal, P., Manjithaya, R., and Surolia, N. (2020). Autophagy-related protein PfATG18 participates in food vacuole dynamics and autophagy-like pathway in Plasmodium falciparum. Mol. Microbiol. *113*, 766–782. https://doi.org/10.1111/mmi.14441.
62. Usui, M., and Williamson, K.C. (2021). Stressed Out About Gametocytogenesis. Front. Cell. Infect. Microbiol. *11*, 790067. https://doi.org/10.3389/fcimb.2021.790067.
63. Yang, T., Yeoh, L.M., Tutor, M.V., Dixon, M.W., McMillan, P.J., Xie, S.C., Bridgford, J.L., Gillett, D.L., Duffy, M.F., Ralph, S.A., et al. (2019). Decreased K13 Abundance Reduces Hemoglobin Catabolism and Proteotoxic Stress, Underpinning Artemisinin Resistance. Cell Rep. *29*, 2917–2928.e5. https://doi.org/10.1016/j.celrep.2019.10.095.
64. Siddiqui, G., Srivastava, A., Russell, A.S., and Creek, D.J. (2017). Multi-omics Based Identification of Specific Biochemical Changes Associated With PfKelch13-Mutant Artemisinin-Resistant Plasmodium falciparum. J. Infect. Dis. *215*, 1435–1444. https://doi.org/10.1093/infdis/jix156.
65. Birnbaum, J., Scharf, S., Schmidt, S., Jonscher, E., Hoeijmakers, W.A.M., Flemming, S., Toenhake, C.G., Schmitt, M., Sabitzki, R., Bergmann, B., et al. (2020). A Kelch13-defined endocytosis pathway mediates artemisinin resistance in malaria parasites. Science *367*, 51–59. https://doi.org/10.1126/science.aax4735.
66. Sinha, A., Hughes, K.R., Modrzynska, K.K., Otto, T.D., Pfander, C., Dickens, N.J., Religa, A.A., Bushell, E., Graham, A.L., Cameron, R., et al. (2014). A cascade of DNA-binding proteins for sexual commitment and development in Plasmodium. Nature *507*, 253–257. https://doi.org/10.1038/nature12970.
67. Brancucci, N.M.B., Bertschi, N.L., Zhu, L., Niederwieser, I., Chin, W.H., Wampfler, R., Freymond, C., Rottmann, M., Felger, I., Bozdech, Z., and Voss, T.S. (2014). Heterochromatin protein 1 secures survival and transmission of malaria parasites. Cell Host Microbe *16*, 165–176. https://doi.org/10.1016/j.chom.2014.07.004.
68. Wang, H., La Russa, M., and Qi, L.S. (2016). CRISPR/Cas9 in Genome Editing and Beyond. Annu. Rev. Biochem. *85*, 227–264. https://doi.org/10.1146/annurev-biochem-060815-014607.
69. Hilton, I.B., D'Ippolito, A.M., Vockley, C.M., Thakore, P.I., Crawford, G.E., Reddy, T.E., and Gersbach, C.A. (2015). Epigenome editing by a CRISPR-Cas9-based acetyltransferase activates genes from promoters and enhancers. Nat. Biotechnol. *33*, 510–517. https://doi.org/10.1038/nbt.3199.

70. Xiao, B., Yin, S., Hu, Y., Sun, M., Wei, J., Huang, Z., Wen, Y., Dai, X., Chen, H., Mu, J., et al. (2019). Epigenetic editing by CRISPR/dCas9 in Plasmodium falciparum. Proc. Natl. Acad. Sci. USA *116*, 255–260. https://doi.org/10.1073/pnas.1813542116.
71. Cheng, A.W., Wang, H., Yang, H., Shi, L., Katz, Y., Theunissen, T.W., Rangarajan, S., Shivalila, C.S., Dadon, D.B., and Jaenisch, R. (2013). Multiplexed activation of endogenous genes by CRISPR-on, an RNA-guided transcriptional activator system. Cell Res. *23*, 1163–1171. https://doi.org/10.1038/cr.2013.122.
72. Xu, L., Zhao, L., Gao, Y., Xu, J., and Han, R. (2017). Empower multiplex cell and tissue-specific CRISPR-mediated gene manipulation with self-cleaving ribozymes and tRNA. Nucleic Acids Res. *45*, e28. https://doi.org/10.1093/nar/gkw1048.
73. Bayat, H., Modarressi, M.H., and Rahimpour, A. (2018). The Conspicuity of CRISPR-Cpf1 System as a Significant Breakthrough in Genome Editing. Curr. Microbiol. *75*, 107–115. https://doi.org/10.1007/s00284-017-1406-8.
74. Swarts, D.C., and Jinek, M. (2018). Cas9 versus Cas12a/Cpf1: Structure-function comparisons and implications for genome editing. Wiley Interdiscip. Rev. RNA *9*, e1481. https://doi.org/10.1002/wrna.1481.
75. Lucky, A.B., Wang, C., Li, X., Chim-Ong, A., Adapa, S.R., Quinlivan, E.P., Jiang, R., Cui, L., and Miao, J. (2023). Characterization of the dual role of Plasmodium falciparum DNA methyltransferase in regulating transcription and translation. Nucleic Acids Res. *51*, 3918–3933. https://doi.org/10.1093/nar/gkad248.
76. Lucky, A.B., Wang, C., Liu, M., Liang, X., Min, H., Fan, Q., Siddiqui, F.A., Adapa, S.R., Li, X., Jiang, R.H.Y., et al. (2023). A type II protein arginine methyltransferase regulates merozoite invasion in Plasmodium falciparum. Commun. Biol. *6*, 659. https://doi.org/10.1038/s42003-023-05038-z.
77. Ghorbal, M., Gorman, M., Macpherson, C.R., Martins, R.M., Scherf, A., and Lopez-Rubio, J.J. (2014). Genome editing in the human malaria parasite Plasmodium falciparum using the CRISPR-Cas9 system. Nat. Biotechnol. *32*, 819–821. https://doi.org/10.1038/nbt.2925.
78. Livak, K.J., and Schmittgen, T.D. (2001). Analysis of relative gene expression data using real-time quantitative PCR and the 2(-Delta Delta C(T)) Method. Methods *25*, 402–408. https://doi.org/10.1006/meth.2001.1262.
79. Deitsch, K., Driskill, C., and Wellems, T. (2001). Transformation of malaria parasites by the spontaneous uptake and expression of DNA from human erythrocytes. Nucleic Acids Res. *29*, 850–853. https://doi.org/10.1093/nar/29.3.850.
80. Jo, H., and Koh, G. (2015). Faster single-end alignment generation utilizing multi-thread for BWA. Bio Med. Mater. Eng. *26*, S1791–S1796. https://doi.org/10.3233/BME-151480.
81. Li, H., Handsaker, B., Wysoker, A., Fennell, T., Ruan, J., Homer, N., Marth, G., Abecasis, G., and Durbin, R.; 1000 Genome Project Data Processing Subgroup (2009). The Sequence Alignment/Map format and SAMtools. Bioinformatics *25*, 2078–2079. https://doi.org/10.1093/bioinformatics/btp352.

STAR★METHODS

KEY RESOURCES TABLE

REAGENT or RESOURCE	SOURCE	IDENTIFIER
Bacterial and virus strains		
XL-blue	Agilent Technologies	Cat#200249
Biological samples		
DiCre/loxP-dCas9-Sir2a	This parasite line was generated in authors' laboratory	N/A
DiCre/loxP-dCas9-GCN5	This parasite line was generated in authors' laboratory.	N/A
Chemicals, peptides, and recombinant proteins		
Chloroquine	Santa Cruz	Cat#sc-207531
Dihydroartemisinin	Sigma-Aldrich	Cat#D7439
Critical commercial assays		
KAPA Hyper prep kit	KAPA Biosystems	Cat#07962363001
Deposited data		
The raw amplicon sequencing data was deposited in Dataverse and can be accessed at https://doi.org/10.7910/DVN/SLRMDN.	Dataverse	N/A
Experimental models: Cell lines		
Plasmodium falciparum 3D7 strain	BEI resources	MRA-151
Oligonucleotides		
Primers for gRNA cloning and RT-PCR (Table S1)	IDT DNA	N/A
Recombinant DNA		
pL6-CS-WR	This vector was modified in authors' laboratory (see details in reference #[31]) based on the vector pL6 (see details in reference #[70])	N/A
Software and algorithms		
FastQC	Babraham Institute	N/A
Trim_galore	Babraham Institute	N/A
Samtools	http://samtools.sourceforge.net	N/A

RESOURCE AVAILABILITY

Lead contact

Further information and requests for resources should be directed to and will be fulfilled by the lead contact, Jun Miao (jmiao1@usf.edu)

Materials availability

This study generated the following new unique reagents: two parasite lines expressing gRNA targeting MDR1 and two parasite pools expressing 10 and 41 gRNAs (see details in Table S1). These reagents are available upon request.

Data and code availability

- Data: All sequencing data that support the findings of this study is publicly available. The raw amplicon sequencing data and detailed sampling and replicate information were deposited in Dataverse and can be accessed at https://doi.org/10.7910/DVN/SLRMDN
- Code: Not applicable.
- Any additional information required to reanalyze the data reported in this work is available from the lead contact upon request.

EXPERIMENTAL MODEL AND STUDY PARTICIPANT DETAILS

This study used *Plasmodium falciparum* 3D7 strain. See the method details section for more information.

METHOD DETAILS

Parasite culture and invasion assays

The *P. falciparum* strain 3D7 and its genetically modified clones were cultured at 37°C in a gas mixture of 5% CO_2, 3% O_2, and 92% N_2 with type O^+ RBCs at 5% hematocrit in RPMI 1640 medium supplemented with 25 mM $NaHCO_3$, 25 mM HEPES, 50 mg/L hypoxanthine, 0.5% Albumax II and 40 mg/ml gentamicin sulfate. Synchronization of asexual stages was performed by sorbitol treatment at the rings stage followed by incubation of synchronized schizonts with fresh RBCs for 3 h to obtain highly synchronized ring-stage parasites. Merozoite invasion assays were conducted according to the established methods.[75,76] Briefly, schizont-infected RBCs were pelleted and resuspended in a culture medium supplemented with 10 μM of the protease inhibitor trans-epoxysuccinyl-l-leucylamido (4-guanidino) butane (E64, Sigma) for 4 h. Merozoites were isolated by mechanically passing schizonts (25% hematocrit) twice through a 1.2 μm-pore-size filter (Whatman) pre-equilibrated with medium. The filtrate containing free merozoites was divided to mix with pre-warmed (37°C) uninfected RBCs, and the number of merozoites contained therein was counted. 24 hours later, the parasitemia of the culture was determined. The invasion rate was calculated as % RBCs invaded × [(RBCs per μl)/ (merozoites per μl)].

Generation of parasite lines regulating MDR1 and RT-PCR

Our lab previously engineered a DiCre/*LoxP* dCas9 HDAC/HAT regulation system targeted to 8 different genes using individual gRNAs.[31] To generate transgenic single parasite clones in both the HDAC and HAT parasite backgrounds targeting *MDR1*. Primers for cloning gRNA targeting 532 bp upstream of start codon (ATG) of *MDR1* (Forward: TAAGTATATAATATTCATGGATATAGAAAGAAAAAG TTTTAGAGCTAGAA and Reverse: TTCTAGCTCTAAAACTTTTTCTTTCTATATCCATGAATATTATATACTTA) were synthesized and cloned into pL6-CS-WR to form pL6-*MDR1*-gRNA by established methods.[31,70,77] The pL6-*MDR1*-gRNA was transfected into parasite lines with inducible dCas9-HAT and -HDAC background.[31] Two primers (Forward: TCAGTATCAAAGAAGAGGTTGAAA and Reverse: ATTTTCTATGTTGTGCAGGTAAAC) were synthesized for analyzing the expression of MDR1 by Reverse transcriptase and real-time PCR (RT-PCR) based on the established methods.[31] Briefly, RT-PCRs were conducted by using SuperScript III RT (Invitrogen) and Faststart Universal SYBR green master mix (Roche). The relative expressions of MDR1 in the rap-induced (+rap) and dimethyl sulfoxide (DMSO)-treated (-rap) parasites were normalized to seryl-tRNA synthetase (PF3D7_0717700) and calculated using the $2-\Delta\Delta CT$ method.[78] The analysis of the expression of the seven tested genes in the parasite pools was conducted as described above using primer pairs listed in Table S1.

Pooling clones for mixed cultivation

Initially, nine single parasite clones with different gRNAs in the HDAC or HAT parasite background were pooled at 0.1% highly synchronous trophozoite stage parasitemia per clone. After 1.5 asexual cycles (at early ring stage), 100 nM rapamycin (+rap) or dimethyl sulfoxide DMSO (-rap) was administered to HDAC and HAT pools overnight to induce expression of the dCas9-fused HDAC/HAT modules. Parasites gDNA were then harvested every day for the first 5 days and then every other day for the next 3 days for a total of 8 collections.

Chloroquine treatment

Therapeutic stress by chloroquine (CQ, sc-207531 Santa Cruz) was supplied daily (without washing out) to synchronous ring-stage HDAC and HAT pools which had grown for 2 cycles after rapamycin treatment (day 4 post-dCas9-fused HDAC/HAT induction). After one cycle of 10 nM CQ treatment, the concentration was increased to 15 nM for 2 cycles where the first gDNA was harvested at the trophozoite stage (day 6 post-initial CQ treatment). Because the parasites did not show any growth defects, CQ was further increased to 20 nM and a final trophozoite gDNA harvest was corrected on day 8 post-CQ treatment.

DHA treatment

Two cycles after rapamycin induction, synchronous ring stage HDAC, and HAT pools were treated with 10 nM dihydroartemisinin (DHA, D7439 Sigma-Aldrich) for 6 hours after which cultures were washed and returned to standard culture conditions. The HDAC pool progressed to the next cycle without noticeable defects. The HAT-rap had unhealthy parasites but apparent death was seen in HAT+rap. On the second cycle (day 3 post-DHA), only the HDAC parasites were given another 6 h, 10 nM DHA pulse. HDAC trophozoite gDNA was harvested 6 days post-DHA treatment. The HAT trophozoites were harvested when sufficient parasitemia was attained at 7 days post-DHA treatment.

Low glucose starvation

Nutritional stress following 2 cycles of rapamycin induction was performed by culturing synchronous ring-stage HDAC and HAT pools in low glucose medium (0.5 g/L for 6 h). Parasites were returned to the normal culture medium to complete the cycle. The same treatment was performed at the subsequent ring stage of cycle 2. For the third cycle, the HDAC and HAT pools were cultured for 8 h in a low-glucose medium. gDNA was harvested on the 3rd cycle (day 6 post initial starvation) at the trophozoite stage.

Heat stress

The dCas9-fused HDAC/HAT was induced with rapamycin and parasites were allowed to grow for 2 cycles before heat shock was applied. Treatment with heat shock at 41°C for 6 h was performed on synchronous ring stage HDAC and HAT pools after which they were returned

to 37°C. The same HS treatment was performed at the subsequent ring stage of cycle 2. For the third cycle, parasites were heat shocked for 8 h before trophozoites stage gDNA was harvested on day 6 post-initial HS.

Transfection of mixed plasmids

Parasite transfection was done using the RBC loading method.[79] Briefly, for the smaller pool of gRNAs (n*n*=10), 10 μg of plasmid /gRNA was introduced into fresh RBCs by electroporation. For the larger pool (*n*=41), 3 μg of plasmid /gRNA was used for electroporation. Purified schizonts were used to infect the RBCs pre-loaded with the plasmid, and selection was done with the drug WR99210 (Jacobus Pharmaceuticals) at 2.5 nM for approximately 4 weeks with weekly replenishment of fresh RBCs until resistant parasites appeared.

Amplicon sequencing

All parasite gDNA was isolated using the ZYMO Quick-DNA™ miniprep kit (Zymo research). To amplify individual gRNA loci on the pL6-CS plasmid,[31,70] PCR was performed with the same amount of gDNA (10 ng) using F1 (CCTATATGCACATATTTCATATTAAG) and R1 (CTTGCTATTTCTAGCTCTAAAAC) primers (Figure 1B). PCR products were separated by agarose gel and stained with ethidium bromide to monitor specific amplification. The amplicons were then used to generate libraries using the KAPA Hyper prep kit for the Illumina sequencing platform according to the manufacturer's protocol (KAPA Biosystems). Pooled libraries were sequenced on the Illumina NextSeq2000 instrument using 150 bp paired-end sequencing and dual indexing. Amplicon-seq was performed to compare the proportion of gRNAs as a proxy to parasite growth during the IDC among the HDAC and HAT pools in normal or stress conditions. The raw amplicon sequencing data and detailed sampling and replicate information were deposited in Dataverse: https://doi.org/10.7910/DVN/SLRMDN.

Amplicon-seq analysis

The initial sequencing reads underwent quality control and adapter trimming processes using FastQC and Trim_galore, respectively, both developed by Babraham Institute. The resultant reads were then aligned to the 50 bp forward and reverse gRNA loci sequences using BWA[80] (Figure 1B). The read count for each gRNA was calculated by 'samtools idxstats'.[81] The read count for each gRNA was then normalized by dividing the read count of each gRNA by the total read count of all gRNAs in each pooled sample and the normalized data was shown as RPM values via a housemade R script (R version 4.2.0). The RPM values were subsequently employed to calculate the fold change between induction (+rap) and un-induction (-rap) for both HAT and HDAC conditions. To exclude the factors caused by the competitive growth in the drug (CQ and DHA) treatment and stress (LG and HS) conditions, additional normalization was designed. That is to divide the fold changes under these conditions by the fold changes in the competitive growth at the same time point. We further calculated the changes between the HAT and HDAC pools by comparing the fold changes between HAT and HDAC. For clarity, we refer to this comparison (fold change) as the "fitness score".

QUANTIFICATION AND STATISTICAL ANALYSIS

To assess the significance of the fitness score, we compared the fold change of each gRNA in the HAT and HDAC pools under normal growth conditions without rapamycin induction. The resulting log2 (fold change) across all time points follows a Gaussian distribution with the majority centered around 0 (Figure S4). We estimated the *p* values of the fitness scores based on this normal distribution using maximum likelihood estimation.